

pubs.acs.org/JACS Article

# Engineering Colloidal Quasi-2D Quantum Wells for High-Performance Room-Temperature Single-Photon Sources

Tingting Yin,\*,<sup>○</sup> Xiao Liang,<sup>○</sup> Yuqing Huang, Yi Tian Thung, Zhenhua Ni,\* Handong Sun,\* and Hilmi Volkan Demir\*



Cite This: J. Am. Chem. Soc. 2025, 147, 34540-34547



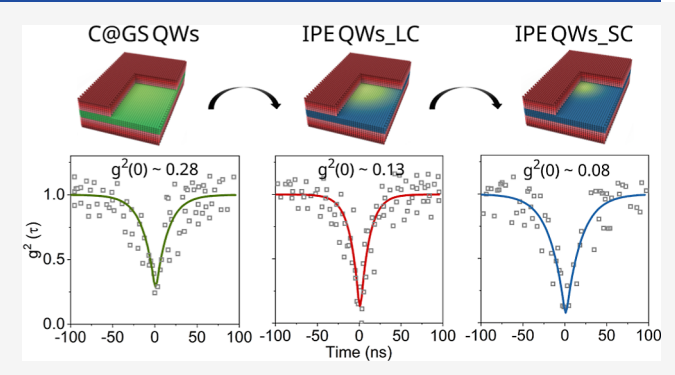
**ACCESS** I

III Metrics & More

Article Recommendations

s Supporting Information

**ABSTRACT:** Single-photon sources (SPSs) are essential for quantum technologies. Colloidal quasi two-dimensional (2D) quantum wells (QWs) possess high emission uniformity, photoluminescence quantum yields (PLQYs), and narrow linewidths at room temperature, all contributing to ideal SPSs. However, their large lateral dimensions make excitons sensitive to environments and enhance multiexciton emission, casting long-standing doubt on their viability as SPSs. Here, we demonstrate bright room-temperature single-photon emission (SPE) with high purity and minimal blinking from in-plane-engineered (IPE) 2D QWs incorporating a doubly gradient architecture. A compositionally graded CdSe/CdSe<sub>x</sub>S<sub>1-x</sub> core in the in-plane direction tailors electron—hole wavefunctions to control multiexciton Auger



dynamics, while a graded  $Cd_yZn_{1-y}S$  shell in the thickness direction suppresses interfacial strain and nonradiative defects. This design unites 0D and 2D structural advantages, achieving near-unity ensemble PLQY and bright SPE  $(0.6-1.2 \times 10^5 \text{ counts/s}, \text{NA} = 0.65)$ . Controlling the CdSe core size via IPE, we attain 92% single-photon purity (2 nm core), and suppressed blinking with a 96.9% ON-time fraction (8 nm core). This work establishes deterministic design rules for colloidal 2D QWs as high-performance SPSs for scalable quantum technologies.

# INTRODUCTION

A high-performance single-photon source with suppressed blinking, high single-photon purity, narrow emission linewidth, and fast emission kinetics at room temperature, is essential for practical applications in the fields of quantum information and quantum communication. 1-6 To date, a variety of colloidal nanomaterials have been developed, such as quasi zerodimensional (0D) quantum dots (QDs), which have been widely studied and demonstrated as the potential nextgeneration single-photon sources. 7,8 For example, lead halide perovskite QDs<sup>9-11</sup> and CdSe-based QDs<sup>12-15</sup> have attracted particular interest due to their exceptional optical properties at room temperature, including high photoluminescence (PL) quantum yield (QY), narrow emission linewidth, short radiative lifetime, facile tunability of the bandgap over a wide range via size, shape, and composition control, low-cost synthesis, and solution processability. Despite decades of advancement, even the most developed colloidal QDs still exhibit size distributions, complicating the understanding of their intrinsic physical mechanisms due to the size-dependent nature of their photophysical properties at the single-particle level. It therefore presents a significant challenge for the onchip integration of 0D QD-based single-photon emitters, which are essential for the development of coherent quantum

light sources. Moreover, the strong quantum confinement from all directions leads to serious nonradiative Auger recombination in 0D QDs, increasing the fluctuations in PL intensity, i.e., blinking. While reducing Auger recombination in the existing systems also tends to increase PL lifetime due to the reduced electrostatic interaction between electrons ( $e^-$ ) and holes ( $h^+$ ), which hampers the realization of quantum and classical photonic technologies relying on high brightness as well as fast communication rates.

A newer class of colloidal nanomaterials, known as quasi two-dimensional (2D) quantum wells (QWs), features a thin platelet geometry with lateral sizes ranging from ~10 to hundreds of nanometers. These QWs exhibit one-dimensional (1D) quantum confinement in the vertical direction, the strength of which can be precisely set at the atomic scale via thickness control. Since the thickness directly determines the emission wavelength, inhomogeneous linewidth broad-

Received: May 24, 2025 Revised: August 20, 2025 Accepted: August 21, 2025 Published: September 11, 2025





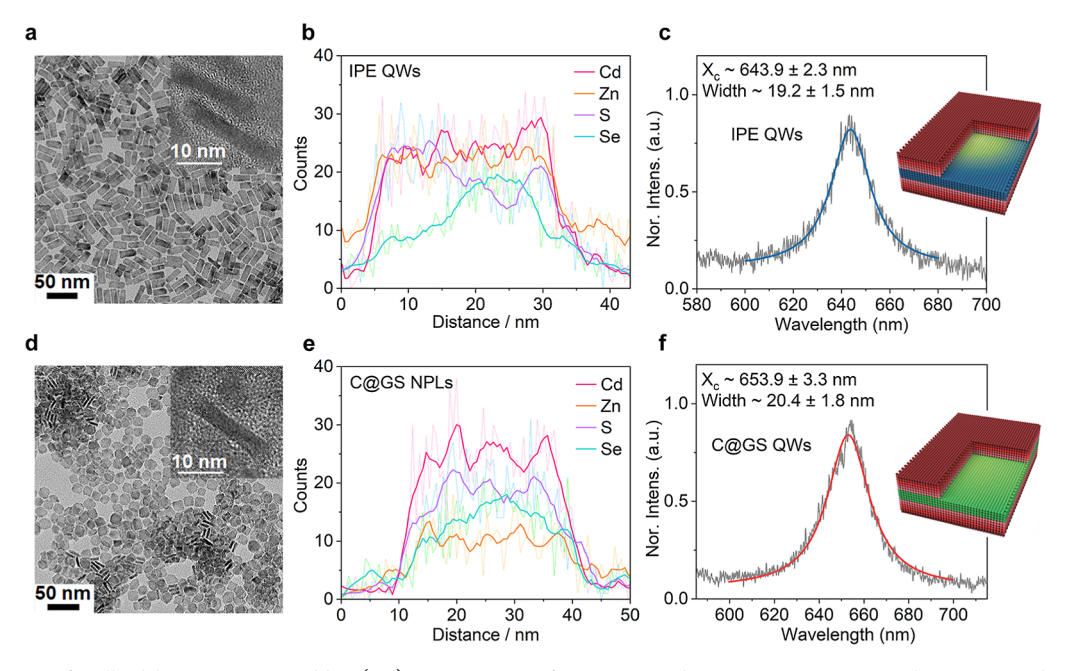


Figure 1. Properties of Colloidal 2D QWs ensembles. (a,d) TEM images of IPE QWs and C@GS QWs, respectively. Insets: High-resolution TEM images. (b,e) EDS line-scan results for the two types of QWs. (c,.f) PL spectra of an IPE QW and C@GS QW. Insets: Schematic representations of crystal structures of the two types of QWs.

ening caused by size variations is effectively eliminated. This leads to narrow emission linewidths and high absorption cross sections. 19,20 Additionally, the large dimensions of QWs facilitate the conversion of excess energy into carrier kinetic energy, thereby their Auger recombination rates are intrinsically low. Colloidal 2D QWs can be prepared with identical thickness, offering spectrally pure emitters suitable for diverse optical applications. Among them, 2D CdX (X = Se, S, Te)based QWs have been demonstrated with high-color purities, large absorption coefficient, and short radiative lifetimes.<sup>21–25</sup> Moreover, the atomically flat nature of 2D QWs enables the fabrication of advanced heterostructures, such as core-shell, core-crown and core-crown-shell. 26-29 These QW heterostructures have been extensively studied for high-performance room-temperature lasing 30-33 and light-emitting diodes (LEDs). 34-36 Despite their promise, the exploration of quantum properties in individual 2D QW heterostructures remains limited. Unlocking their potential as candidates for quantum information and quantum communication applications is therefore an urgent research priority. To date, only a few studies have reported single-photon emission from individual 2D QWs at room temperature, and their emission properties have been suboptimal. For example, single 2D CdSe QWs exhibit severe blinking behavior with emission intensity comparable to background noise.<sup>37</sup> Similarly, core/shell CdSe/ ZnS QWs have shown long-period blinking and bleaching.

In this work, we report a significant breakthrough in achieving bright room-temperature single-photon emission from a novel architecture of in-plane-engineered (IPE) 2D QW heterostructures. These structures combine an in-plane compositional gradient core of  $CdSe/CdSe_xS_{1-x}$  and an out-of-plane graded alloyed  $Cd_yZn_{1-y}S$  shell. The doubly gradient (DG) architecture enables the IPE QWs (with a CdSe seed size of ~8 nm) to exhibit stable ensemble PL with a near-unity PLQY exceeding 99%. At single-particle level, individual IPE QWs demonstrate an average  $g^{(2)}(0)$  value of 0.15  $\pm$  0.04, alongside effectively suppressed blinking, with a high average

ON-time fraction of 95  $\pm$  1.9%. Furthermore, the DG structure allows precise tuning of the exciton concentration within the CdSe seed by controlling the relative size of the seed to the overall lateral size of the QW. This tunability enables the optimization of single exciton radiative recombination rates as well as nonradiative Auger recombination rates. By engineering the gradient core with a CdSe seed size of  $\sim$ 2 nm, we achieved a high single-photon purity of  $\sim$ 92%, corresponding to a  $g^{(2)}(0)$  value as low as  $\sim$ 0.08. These results represent a significant advancement toward the realization of robust room-temperature quantum emission based on the emerging colloidal 2D QW system.

# RESULTS AND DISCUSSION

**2D IPE QWs.** The inset in Figure 1c schematically illustrates the structure of the IPE QWs studied in this work. The preparation of the IPE QWs begins with the synthesis of a gradient core, involving the growth of 4-monolayer CdSe seeds. Once the CdSe seeds reach the desired size, sulfur (S) precursors were consistently introduced, resulting in a lateral transition from CdSe to CdS due to the continuous consumption of selenide (Se) and the injection of S precursors. The morphology and composition of the gradient core were characterized using spherical aberration-corrected transmission electron microscopy (TEM), energy-dispersive X-ray spectroscopy (EDS) mapping and line-scan characterizations, as shown in Figure S1. Subsequently, the graded alloyed Cd<sub>v</sub>Zn<sub>1-v</sub>S shell was grown by leveraging differences in the reaction rates of zinc, cadmium and S precursors.<sup>39</sup> This sequential reaction enables the graded transformation from CdS to ZnS along the vertical direction, as confirmed by EDS mapping results from spherical aberration-corrected TEM (Figure S2). The typical structural information on the final IPE QWs products were revealed in Figure S3. For comparison, conventional core@ gradient shell (C@GS) QWs were also synthesized, with their structural schematic shown in the inset of Figure 1f. TEM images of both IPE and C@GS QWs (Figure 1a,d) reveal

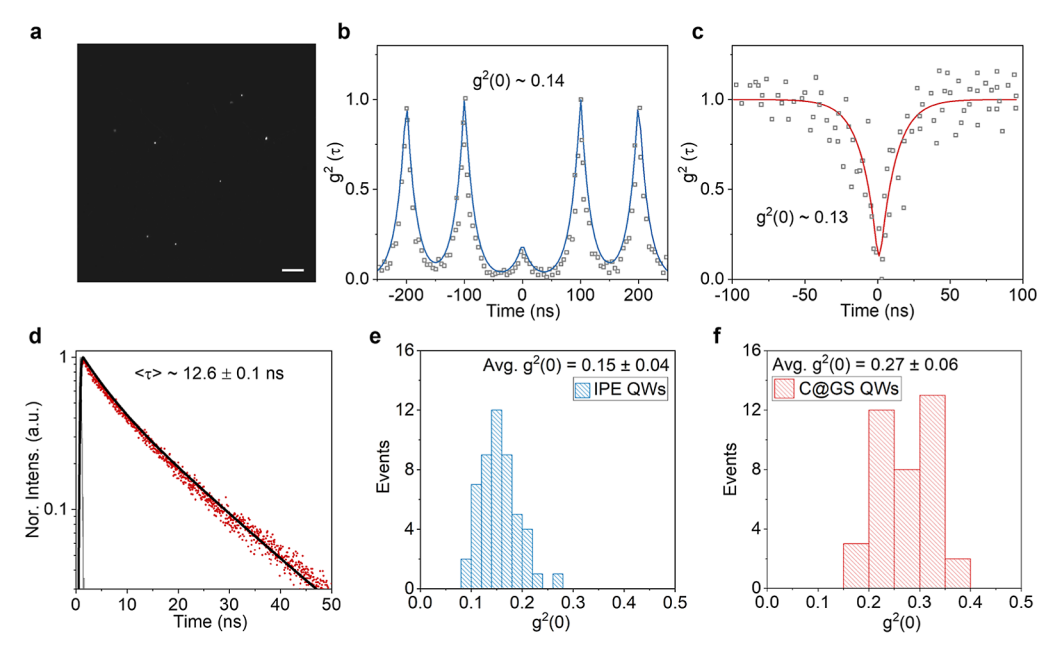


Figure 2. Single-photon purity of single 2D IPE QWs. (a) Wide-field illumination image of isolated QWs excited by a 470 nm LED. The scale bar is 10 μm. Second-order PL intensity correlation functions measured under (b) pulsed excitation and (c) CW excitation at 470 nm with an excitation power of 2.5 W/cm<sup>2</sup>. (d) PL decay profile (red dots) of a VEE QW and the corresponding fitted curve (black line). Inset: Mean PL lifetime ( $\langle \tau \rangle$ ) obtained from measurements of 50 VEE QWs. Histograms of the  $g^{(2)}(0)$  distribution for 50 VEE QWs (e) and 50 C@GS QWs (f).

highly uniform lateral sizes and shell thicknesses for the IPE QWs compared to the C@GS QWs. EDS line-scan results (Figure 1b,e) further highlight a key structural difference between IPE and C@GS QWs: the in-plane size of the CdSe core. The CdSe core in IPE QWs measures approximately 8 nm along the long axis, while in C@GS QWs, the CdSe core size is around 20 nm. PL spectra of single IPE QWs show an average emission peak at  $643.9 \pm 2.3$  nm with a linewidth of  $19.2 \pm 1.5$  nm, based on measurements of 50 QWs. Single C@ GS QWs exhibit an average emission peak at 653.9  $\pm$  3.3 nm with a linewidth of  $20.4 \pm 1.8$  nm, determined from 50 QWs. For comparison, the ensemble emission linewidths are measured at 20.8  $\pm$  0.1 nm for IPE QWs and 20.0  $\pm$  0.2 nm for C@GS QWs (Figure S4). The strong spectral correlation between single QWs and their ensembles highlights the dominant role of 1D quantum confinement in 2D QWs with lateral sizes exceeding 10 nm. This confinement ensures that variations in the other two dimensions have negligible effects on the optical properties, underscoring the unique advantages of this system. Moreover, the PLQYs of all studied QW ensembles exceed 99% (Figure S5). The exceptional properties underscore the immense potential of 2D IPE QWs as efficient single-photon emitters, warranting further exploration of their room-temperature emission performance at the single-particle level.

Single-Photon Emission from Individual 2D IPE QWs. The single-photon purity of individual 2D IPE QWs was evaluated through second-order photon correlation function  $g^{(2)}(\tau)$  measurements. Figure 2a shows a wide-field illumination image of the IPE QW dispersion, where each bright spot corresponds to the fluorescence from an individual IPE QW. Under pulsed laser excitation at 475 nm, the  $g^{(2)}(0)$  value was calculated to be  $\sim$ 0.14, representing the average area ratio between the central and the four side peaks (Figure 2b). This result aligns with the value of  $\sim$ 0.13 obtained under continuous-wave (CW) excitation at the same wavelength

(Figure 2c). The mean lifetime of individual IPE QWs was determined to be  $12.6 \pm 0.1$  ns (Figure 2d), which was based on measurements of 50 QWs. To provide statistical insight,  $g^{(2)}(\tau)$  measurements were conducted on 50 IPE QWs, and a histogram of  $g^{(2)}(0)$  distributions is presented in Figure 2e. The averaged  $g^{(2)}(0)$  value for IPE QWs is 0.15  $\pm$  0.04, significantly lower than the averaged  $g^{(2)}(0)$  value of 0.27  $\pm$ 0.06 obtained for C@GS QWs (as determined from 50 C@GS QWs). This lower  $g^{(2)}(0)$  value for IPE QWs reflects their superior single-photon purity, 9,40,41 indicating effective suppression of multiexciton emission in the IPE QWs studied here. To further investigate the nonradiative Auger recombination rate of multiexcitons, power-dependent transient absorption (TA) spectroscopy was performed on these QW ensembles (Figure S6a-c). A fast decay component, characteristic of Auger recombination, was observed in the TA spectra of these QWs. Notably, the nonradiative Auger component in IPE QWs exhibits a faster rate at all pump fluences compared to C@GS QWs (Figure S6c), coinciding with the high singlephoton purity observed in 2D IPE QWs.

Minimum Blinking in Single 2D IPE QWs. To investigate the PL blinking behavior of individual IPE QWs, we recorded the PL intensity time traces of both single IPE QWs and C@GS QWs under pulsed laser excitation at 470 nm. PL intensity time trace of an IPE QW is presented in Figure 3a (left panel), with the corresponding histogram of PL intensity distribution shown in the right panel. The blinking is very limited and follows a simple ON/OFF pattern, without any GREY-state emission. Notably, the ON-time fraction for the selected IPE QW is 95.9%, with an average ON-time fraction of 95.0  $\pm$  1.9%. Additional PL intensity time traces of other IPE QWs are provided in Figure S7. For comparison, we measured the PL intensity time trace of single C@GS QWs, as illustrated in Figures 3d and S8. Unlike the IPE QWs, the C@ GS QWs exhibit three blinking states: ON, GREY and OFF. The ON-time fraction in a C@GS QW decreases to 54.8%,

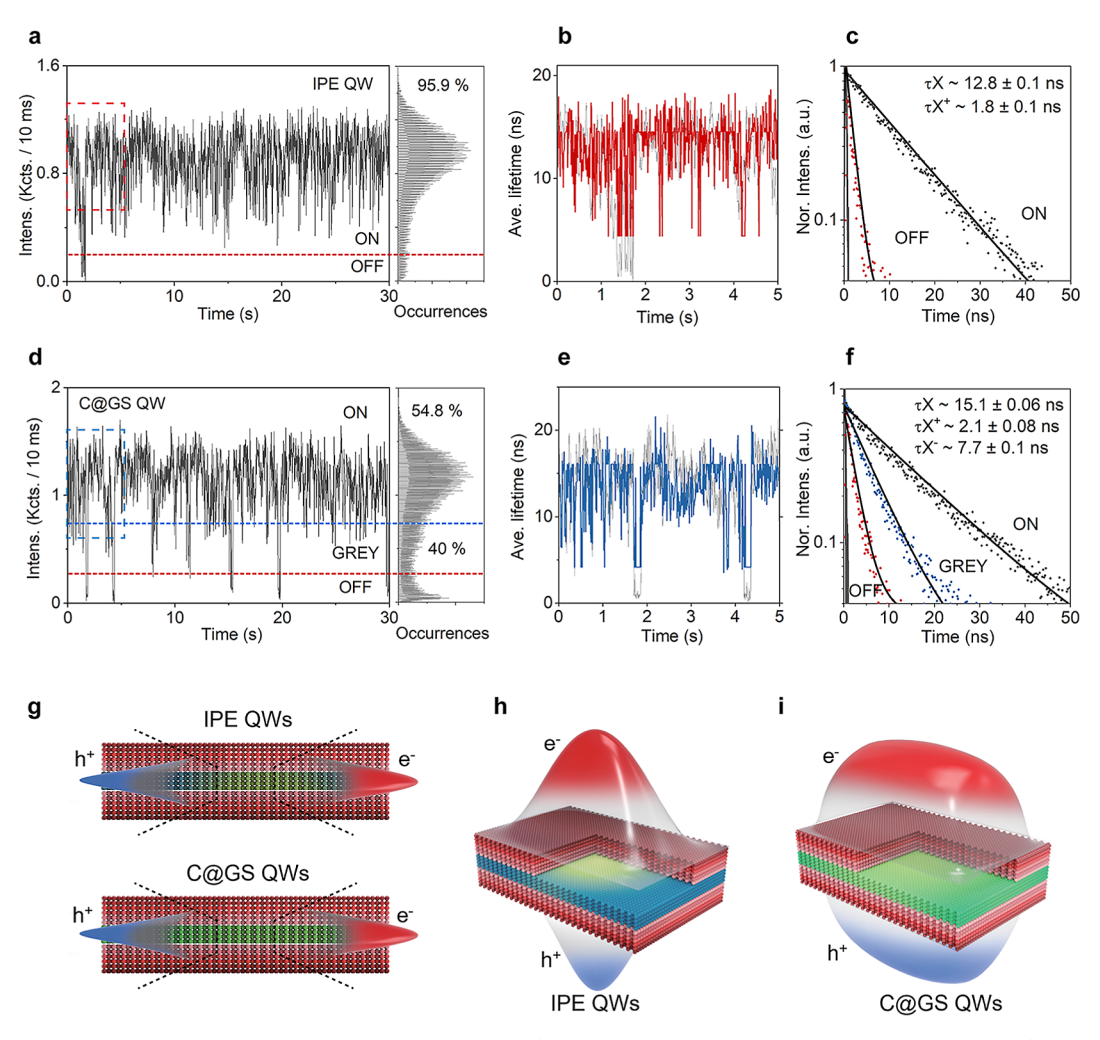


Figure 3. Blinking behaviors of single IPE QWs and C@GS QWs. (a,d) Representative PL intensity trajectories (black lines) of an IPE QW and C@GS QW (left panels), with corresponding histograms (grey) shown in the right panels. The bin time is 10 ms. Dashed red and blue lines indicate thresholds between ON, GREY and OFF states, used for calculating the ON-time fraction. (b,e) PL intensity (back lines) and average lifetime (colored lines) for selected 5 s time regions (colored dashed boxes) from (a) and (d). (c,f) PL decay curves of the ON (black dots), GREY (blue dots) and OFF (red dots) states corresponding to (a) and (d).  $\tau X$ ,  $\tau X^+$  and  $\tau X^-$  represent the decay times of neutral excitons, positive trions and negative trions, respectively. Solid black lines are monoexponential fits, while solid grey lines represent the instrument response function (IRF) of the system. (g) Schematic representation of potential barriers and e<sup>-</sup> and h<sup>+</sup> wavefunctions along the out-of-plane direction for IPE QWs (top) and C@GS QWs (bottom), respectively. (h,i) Schematic representations of e<sup>-</sup> and h<sup>+</sup> wavefunctions along the in-plane direction for IPE QWs (h) and C@GS QWs (i), respectively.

with an average ON-time fraction of  $63.2 \pm 5.2\%$  (refer to Figure S9 for details), reflecting a significant decrease in the time spent in the ON state. To further analyze the blinking behavior, we selected short intervals (5 s) from the PL intensity trajectories of both QWs, as indicated by the red dashed box in Figure 3a and the blue dashed box in Figure 3d. These intervals are shown alongside the average PL lifetime trajectories (red and blue lines) for individual IPE QWs (Figure 3b) and C@GS QWs (Figure 3e). The average lifetime was calculated by taking a weighted average of the decay time histogram. A clear correlation between the PL intensity fluctuations (ON/OFF) and the average lifetime observed in both QWs indicates A-type blinking, which is attributed to the charging-induced Auger recombination.

The PL decay dynamics for different emission states were extracted from the PL intensity trajectories. The ON state, attributed to neutral excitons, exhibits lifetimes of  $12.8 \pm 0.1$  ns for an IPE QW and  $15.0 \pm 0.06$  ns for a C@GS QW, as indicated by the black dots in Figure 3c,f. In contrast, the OFF

state for both QWs shows comparably short lifetimes of 1.8  $\pm$  0.1 ns and 2.1  $\pm$  0.08 ns, respectively (the red dots in Figure 3c,f), which should be from the same charged exciton state. 45,46 Interestingly the GREY state observed in a C@ QWs shows a slightly longer lifetime of 7.6  $\pm$  0.1 ns (the blue dots in Figure 3f), which likely originates from a different type of charged exciton state. 21,45

To further understand the physical origin of the observed ON, GREY and OFF states in these QWs, we examined the differences in their microscopic structures between IPE QWs and C@GS QWs, as illustrated in Figure 3g–i. Both IPE and C@GS QWs share a similar gradient shell composition along the out-of-plane direction, the  ${\rm e}^-$  and  ${\rm h}^+$  wavefunctions in both cases are confined within the CdSe layer along this direction. This confinement is due to the large energy difference between the conduction and valence bands of CdSe and CdyZn<sub>1-y</sub>S, as depicted in Figure 3g. However, the in-plane spatial distributions of the  ${\rm e}^-$  and  ${\rm h}^+$  wavefunctions differ significantly between IPE QWs and C@GS QWs. In IPE QWs, the  ${\rm e}^-$  and

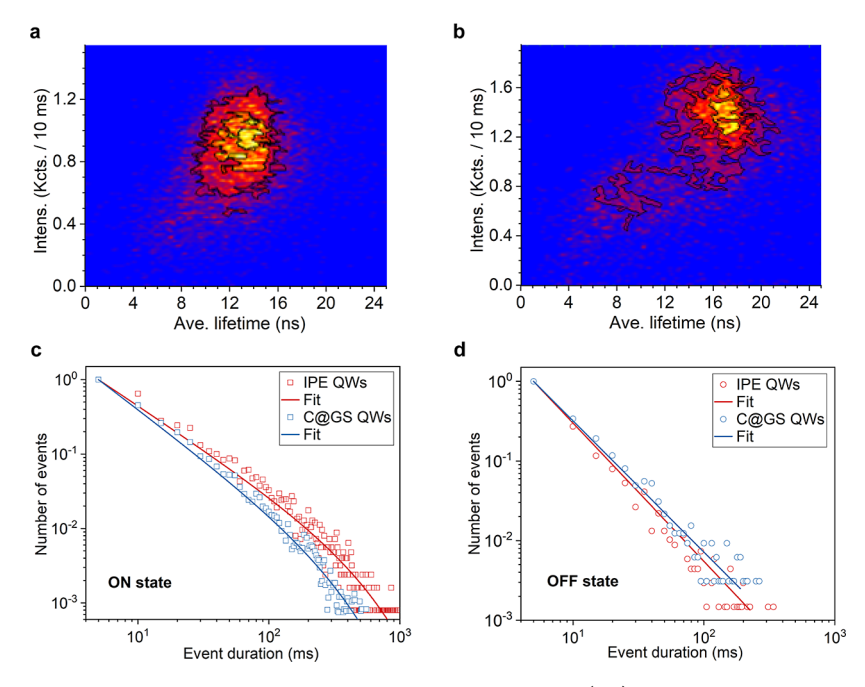


Figure 4. Statistics for ON and OFF times for single 2D IPE QWs and C@GS QWs. (a,b) FLID histograms of an IPE QW and C@GS QW, respectively. (c,d) Statistics of ON- and OFF-time durations in an IPE QW and C@GS QW plotted in the log-log representation. The raw data have been normalized to 1 for ease of comparison.

h<sup>+</sup> wavefunctions are highly localized at the CdSe center of the gradient core (Figure 3h) due to the relatively large band offsets between CdSe and CdS. In contrast, the e<sup>-</sup> and h<sup>+</sup> wavefunctions in C@GS QWs are more delocalized, as shown in Figure 3i. The difference in wavefunction overlap has important implications for the radiative recombination rate of neutral excitons. In IPE QWs, the enhanced overlap of the e and h+ wavefunctions leads to a faster radiative recombination rate. Additionally, the stronger confinement of the h<sup>+</sup> in the core center, compared to the e-, facilitates the formation of positive trions. The OFF state observed in both IPE QWs and C@GS QWs can therefore be attributed to the Auger decay of the positive trions. Meanwhile, the GREY state observed in C@GS QWs, characterized by a slightly longer lifetime, likely originates from the Auger decay of negative trions. This interpretation aligns with previous studies indicating that the Auger rates of positive trions is faster than that of negative trions in II-VI quantum dots.<sup>16</sup> Notably, this GREY-state emission is completely suppressed in 2D IPE QWs, consistent with the high ON-time fraction measured for exciton emission (Figure 3a).

High ON-Time Fraction in Single 2D IPE QWs. Figure 4a, b show the fluorescence-lifetime-intensity distribution (FLID) plots for IPE QWs and C@GS QWs, respectively. Both plots show a clear correlation between the average lifetime and PL intensity, consistent with the behavior of A-type blinking. However, the occurrence probabilities of the OFF states are too small in both QWs to generate sufficient photon statistics for the FLID plots. Specifically, in the case of an IPE QW, the OFF state is not prominent and even appears to "disappear" in the FLID plot, while the ON state dominates with longer durations and high emission intensities. This observation aligns with the higher ON-time fraction observed for single IPE QWs. In contrast, a clear signal corresponding to the GREY state appears at shorter lifetimes in the FLID plot of a C@GS QW. To further compare the A-type blinking

behavior, we performed a detailed statistical analysis of the probability distributions of the durations of ON and OFF events derived from the PL intensity trajectories. The results for an IPE QW and a C@GS QW are shown in Figure 4c,d. In the log-log plots, the ON-time probability distributions exhibit a rapid falloff at longer times, which is well-fitted by a truncated power-law function:  $P_{\text{on}}(t) = A_{\text{on}} t^{-\alpha_{\text{on}}} \exp(-t/\tau)$ ( $\alpha_{\rm on}$  is the power-law exponent of ON state, and  $\tau$  represents the cutoff time),  $^{42,47-51}$  as represented by the solid red and blue lines in Figure 4c. In contrast, the OFF-time durations show nearly linear behavior, which can be well described by a power-law distribution over nearly three decades:  $P_{\rm off}(t) = A_{\rm off} t^{-\alpha_{\rm off}}$  ( $\alpha_{\rm off}$  is the power-law exponent of OFF state), 42,47-51 as represented by the solid red and blue lines in Figure 4d. The averaged fitting parameters  $1/\tau$  and  $\alpha$  were obtained by fitting 50 IPE QWs and 50 C@GS QWs, respectively. The  $\alpha_{\rm on}({\rm IPE})$  is 1.1  $\pm$  0.03 and  $\alpha_{\rm on}({\rm C}@{\rm GS})$  is 1.3  $\pm$  0.04. The  $\alpha_{\rm off}({\rm IPE})$  is 1.8  $\pm$  0.09 and  $\alpha_{\rm off}({\rm C@GS})$  is 1.6  $\pm$ 0.1. The slow decay of the ON time distribution and the fast decay of the OFF time distribution indicate that blinking in our 2D QWs is dominated by long ON events and short OFF event. Notably, IPE QWs possess a smaller  $\alpha_{\rm on}$  and a larger  $\alpha_{\text{off}}$  consistent with the observed high ON-time fraction.

Achieving pure single-photon emission at room temperature is essential for advancing various quantum technologies, which requires the rational design of single-photon emitters. The novel DG structure of our 2D QWs enables precise control over the exciton concentration within the CdSe seed by adjusting the seed size relative to the overall lateral dimension of the QW. This tunability allows for the optimization of single exciton radiative recombination rates. To this end, we engineered IPE QWs with a reduced CdSe seed size of ~2 nm, referred to as IPE QWs with a smaller seed size (IPE QWs\_SSS). These QWs exhibit a high single-photon purity of ~92%, corresponding to a  $g^{(2)}(0)$  value as low as ~0.08, as shown in Figure 5a,b. Detailed structural characterizations and

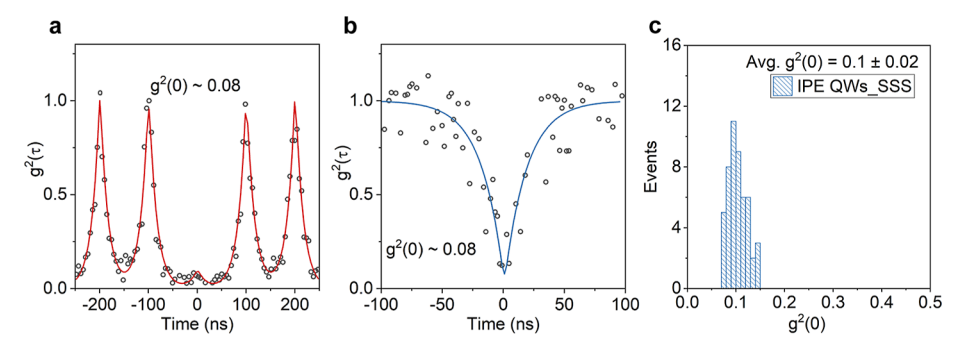


Figure 5. Single-photon purity of an IPE QW\_SSS. Second-order PL intensity correlation functions measured under (a) pulsed excitation and (b) CW excitation at 470 nm with an excitation power of 2.5 W/cm<sup>2</sup>. (c) Histogram of the  $g^{(2)}(0)$  distribution derived from measurements of 50 QWs.

optical properties of IPE QWs\_SSS are provided in Figure S10a—c. A statistical analysis of  $g^{(2)}(0)$  values across 50 QWs is shown in Figure 5c, yielding an average  $g^{(2)}(0)$  of  $0.1 \pm 0.02$ . Furthermore, the PL blinking of single IPE QWs\_SSS is classified as A-type blinking, with an ON-time fraction of ~90% (Figure S11).

# CONCLUSIONS

In summary, we have, for the first time, demonstrated roomtemperature single-photon emission from individual colloidal quasi 2D IPE QWs with a DG architecture. Individual IPE QWs with a CdSe core size of  $\sim$ 8 nm exhibit an average  $g^{(2)}(0)$ value of  $0.15 \pm 0.04$  and a remarkably high ON-time fraction of 95  $\pm$  1.9%, underscoring their purity and stability as quantum emitters. Further optimization of the gradient core structure by reducing the CdSe seed size to ~2 nm leads to a high single-photon purity of ~92%, corresponding to a  $g^{(2)}(0)$ value as low as ~0.08. Our in-depth investigation into the blinking behavior and its underlying physical origins reveal that the gradual compositional transition in both the in-plane and out-of-plane directions of the DG architecture plays a crucial role in effectively passivating surface defects, mitigating straininduced crystal defects, and precisely controlling the spatial overlap of e and h wavefunctions. This unique combination results in 2D IPE QWs with a high ON-time fraction, minimal blinking, and a simple ON/OFF pattern without intermediate GREY state emission. The insights gained from this study enhance our understanding of the photophysics underlying single-photon emission in colloidal 2D QWs. Our findings establish that colloidal 2D QWs are a promising single-photon source platform at room temperature, with great potential to simultaneously satisfy the balance of high uniformity, high PLQYs, narrow emission linewidths, and significantly suppressed blinking. Furthermore, the on-chip integration of 2D QW-based single-photon sources offers a potential breakthrough in addressing the limitations of conventional 0D QDbased single-photon emitters, thereby advancing the development of coherent quantum light sources for quantum technologies.

#### ASSOCIATED CONTENT

# Supporting Information

The Supporting Information is available free of charge at https://pubs.acs.org/doi/10.1021/jacs.5c08797.

> Methods section and experimental details: synthesis of 2D QW heterostructures; structural characterizations; optical characterization of 2D QW ensembles and

individual 2D QWs; supplementary figures; additional results and data; references (PDF)

## AUTHOR INFORMATION

#### **Corresponding Authors**

Tingting Yin - School of Physics and Key Laboratory of Quantum Materials and Devices of Ministry of Education, Southeast University, Nanjing 211189, China; Division of Physics and Applied Physics, School of Physical and Mathematical Sciences, Nanyang Technological University, Singapore 637371, Singapore; orcid.org/0000-0001-9439-3842; Email: ttyin@seu.edu.cn

Zhenhua Ni - School of Physics and Key Laboratory of Quantum Materials and Devices of Ministry of Education, Southeast University, Nanjing 211189, China; School of Electronic Science and Engineering, Southeast University, Nanjing 210096, China; o orcid.org/0000-0002-6316-2256; Email: zhni@seu.edu.cn

Handong Sun – Institute of Applied Physics and Materials Engineering, University of Macau, Macau SAR 999078, P. R. China; orcid.org/0000-0002-2261-7103; Email: hdsun@um.edu.mo

Hilmi Volkan Demir – Division of Physics and Applied Physics, School of Physical and Mathematical Sciences, Nanyang Technological University, Singapore 637371, Singapore; LUMINOUS! Center of Excellence for Semiconductor Lighting and Displays, School of Electrical and Electronic Engineering, School of Physical and Mathematical Sciences, School of Materials Science and Engineering, Nanyang Technological University, Singapore 639798, Singapore; UNAM—Institute of Materials Science and Nanotechnology, The National Nanotechnology Research Center, Department of Electrical and Electronics Engineering, Department of Physics, Bilkent University, Bilkent, Ankara 06800, Turkey; orcid.org/0000-0003-1793-112X; Email: hvdemir@ntu.edu.sg

### **Authors**

Xiao Liang - LUMINOUS! Center of Excellence for Semiconductor Lighting and Displays, School of Electrical and Electronic Engineering, School of Physical and Mathematical Sciences, School of Materials Science and Engineering, Nanyang Technological University, Singapore 639798, Singapore

Yuqing Huang — State Key Laboratory of Semiconductor Physics and Chip Technologies, Institute of Semiconductors, Chinese Academy of Sciences, Beijing 100083, China; College of Materials Science and Optoelectronic Technology,

- University of Chinese Academy of Science, Beijing 100049, China
- Yi Tian Thung Division of Physics and Applied Physics, School of Physical and Mathematical Sciences, Nanyang Technological University, Singapore 637371, Singapore

Complete contact information is available at: https://pubs.acs.org/10.1021/jacs.5c08797

#### **Author Contributions**

<sup>O</sup>T.Y. and X.L. contributed equally to this work.

#### **Funding**

This work is supported by the National Key R&D Program of China 2021YFA1200700. T.Y. acknowledges support from the Natural Science Foundation of Jiangsu Province (SBK20250400377), the Start-up Research Fund of Southeast University (RF1028625090), the open research fund of Key Laboratory of Quantum Materials and Devices of Ministry of Education, Southeast University, and the Presidential Postdoctoral Fellowship at Nanyang Technological University. H.S. acknowledges the Science and Technology Development Fund (FDCT), Macau SAR (0122/2023/RIA2), MOE-Tier 1-RG 139/22, NRF-CRP23-2019-0007, SRG2023-00025, CPG2023-00039 and CPG2025-00034-IAPME. H.V.D. and X.L. acknowledge financial support from the National Research Foundation, Singapore, under its NRF Investigatorship programme (NRF-NRFI10-2024-0003), the Singapore Agency for Science, Technology and Research (A\*STAR) MTC program (Grant No. M21J9b0085). H.V.D. also acknowledges the TUBA and TUBITAK 2247-A National Leader Researchers Program (121C266).

The authors declare no competing financial interest.

# ACKNOWLEDGMENTS

The authors acknowledge the Facility for Analysis, Characterization, Testing and Simulation (FACTS) at Nanyang Technological University, Singapore, and Dr. Tay Yee Yan, for the valuable and professional technical supports in TEM characterizations. The authors also acknowledge partial support for optical measurements from the Center for Fundamental and Interdisciplinary Sciences of Southeast University.

# REFERENCES

- (1) Aharonovich, I.; Englund, D.; Toth, M. Solid-state single-photon emitters. Nat. Photonics 2016, 10 (10), 631-641.
- (2) Aharonovich, I.; Castelletto, S.; Simpson, D. A.; Su, C. H.; Greentree, A. D.; Prawer, S. Diamond-based single-photon emitters. Rep. Prog. Phys. 2011, 74 (7), 076501.
- (3) Senellart, P.; Solomon, G.; White, A. High-performance semiconductor quantum-dot single-photon sources. Nat. Nanotechnol. **2017**, *12* (11), 1026–1039.
- (4) Tomm, N.; Javadi, A.; Antoniadis, N. O.; et al. A bright and fast source of coherent single photons. Nat. Nanotechnol. 2021, 16 (4),
- (5) Sapienza, L.; Davanço, M.; Badolato, A.; Srinivasan, K. Nanoscale optical positioning of single quantum dots for bright and pure single-photon emission. Nat. Commun. 2015, 6 (1), 7833.
- (6) Wang, H.; He, Y.-M.; Chung, T. H.; et al. Towards optimal single-photon sources from polarized microcavities. Nat. Photonics **2019**, 13 (11), 770–775.
- (7) Santori, C.; Pelton, M.; Solomon, G.; Dale, Y.; Yamamoto, Y. Triggered single photons from a quantum dot. Phys. Rev. Lett. 2001, 86 (8), 1502–1505.

- (8) Morozov, S.; Pensa, E. L.; Khan, A. H.; Polovitsyn, A.; Cortes, E.; Maier, S. A.; Vezzoli, S.; Moreels, I.; Sapienza, R. Electrical control of single-photon emission in highly charged individual colloidal quantum dots. Sci. Adv. 2020, 6 (38), No. eabb1821.
- (9) Zhu, C.; Marczak, M.; Feld, L.; et al. Room-temperature, highly pure single-photon sources from all-inorganic lead halide perovskite quantum dots. Nano Lett. 2022, 22 (9), 3751-3760.
- (10) Park, Y.-S.; Guo, S.; Makarov, N. S.; Klimov, V. I. Room temperature single-photon emission from individual perovskite quantum dots. ACS Nano 2015, 9 (10), 10386-10393.
- (11) Castelletto, S.; De Angelis, F.; Boretti, A. Prospects and challenges of quantum emitters in perovskites nanocrystals. Appl. Mater. Today 2022, 26, 101401.
- (12) Galland, C.; Ghosh, Y.; Steinbrück, A.; Hollingsworth, J. A.; Htoon, H.; Klimov, V. I. Lifetime blinking in nonblinking nanocrystal quantum dots. Nat. Commun. 2012, 3 (1), 908.
- (13) Javaux, C.; Mahler, B.; Dubertret, B.; et al. Thermal activation of non-radiative Auger recombination in charged colloidal nanocrystals. Nat. Nanotechnol. 2013, 8 (3), 206-212.
- (14) Chen, O.; Zhao, J.; Chauhan, V. P.; et al. Compact high-quality CdSe-CdS core-shell nanocrystals with narrow emission linewidths and suppressed blinking. Nat. Mater. 2013, 12 (5), 445-451.
- (15) Lin, X.; Dai, X.; Pu, C.; Deng, Y.; Niu, Y.; Tong, L.; Fang, W.; Jin, Y.; Peng, X. Electrically-driven single-photon sources based on colloidal quantum dots with near-optimal antibunching at room temperature. Nat. Commun. 2017, 8 (1), 1132.
- (16) Hou, X.; Kang, J.; Qin, H.; Chen, X.; Ma, J.; Zhou, J.; Chen, L.; Wang, L.; Wang, L. W.; Peng, X. Engineering Auger recombination in colloidal quantum dots via dielectric screening. Nat. Commun. 2019, 10 (1), 1750.
- (17) Ithurria, S.; Dubertret, B. Quasi 2D colloidal CdSe platelets with thicknesses controlled at the atomic level. J. Am. Chem. Soc. 2008, 130 (49), 16504-16505.
- (18) Joo, J.; Son, J. S.; Kwon, S. G.; Yu, J. H.; Hyeon, T. Lowtemperature solution-phase synthesis of quantum well structured CdSe nanoribbons. J. Am. Chem. Soc. 2006, 128 (17), 5632-5633.
- (19) Ithurria, S.; Tessier, M. D.; Mahler, B.; Lobo, R. P. S. M.; Dubertret, B.; Efros, A. L. Colloidal nanoplatelets with twodimensional electronic structure. Nat. Mater. 2011, 10 (12), 936-
- (20) Bouet, C.; Tessier, M. D.; Ithurria, S.; Mahler, B.; Nadal, B.; Dubertret, B. Flat colloidal semiconductor nanoplatelets. Chem. Mater. 2013, 25 (8), 1262-1271.
- (21) Guzelturk, B.; Pelton, M.; Olutas, M.; Demir, H. V. Giant modal gain coefficients in colloidal II-VI nanoplatelets. Nano Lett. **2019**, 19 (1), 277–282.
- (22) Shendre, S.; Delikanli, S.; Li, M.; et al. Ultrahigh-efficiency aqueous flat nanocrystals of CdSe/CdS@Cd<sub>1-x</sub>Zn<sub>x</sub>S colloidal core/ crown@alloyed-shell quantum wells. Nanoscale 2019, 11 (1), 301-
- (23) Kormilina, T. K.; Cherevkov, S. A.; Fedorov, A. V.; Baranov, A. V. Cadmium chalcogenide nano-heteroplatelets: Creating advanced nanostructured materials by shell growth, substitution, and attachment. Small 2017, 13 (41), 1702300.
- (24) Yu, J.; Chen, R. Optical properties and applications of twodimensional CdSe nanoplatelets. InfoMat 2020, 2 (5), 905-927.
- (25) Shabani, F.; Dehghanpour Baruj, H.; Yurdakul, I.; Delikanli, S.; Gheshlaghi, N.; Isik, F.; Liu, B.; Altintas, Y.; Canımkurbey, B.; Demir, H. V. Deep-red-emitting colloidal quantum well light-emitting diodes enabled through a complex design of core/crown/double shell heterostructure. Small 2022, 18 (8), 2106115.
- (26) Pedetti, S.; Ithurria, S.; Heuclin, H.; Patriarche, G.; Dubertret, B. Type-II CdSe/CdTe core/crown semiconductor nanoplatelets. J. Am. Chem. Soc. 2014, 136 (46), 16430-16438.
- (27) Kelestemur, Y.; Guzelturk, B.; Erdem, O.; Olutas, M.; Gungor, K.; Demir, H. V. Platelet-in-box colloidal quantum wells: CdSe/ CdS@CdS core/crown@shell heteronanoplatelets. Adv. Funct. Mater. **2016**, 26 (21), 3570–3579.

- (28) Kelestemur, Y.; Olutas, M.; Delikanli, S.; Guzelturk, B.; Akgul, M. Z.; Demir, H. V. Type-II colloidal quantum wells: CdSe/CdTe core/crown heteronanoplatelets. *J. Phys. Chem. C* **2015**, *119* (4), 2177–2185.
- (29) Tessier, M. D.; Spinicelli, P.; Dupont, D.; Patriarche, G.; Ithurria, S.; Dubertret, B. Efficient exciton concentrators built from colloidal core/crown CdSe/CdS semiconductor nanoplatelets. *Nano Lett.* **2014**, *14* (1), 207–213.
- (30) She, C.; Fedin, I.; Dolzhnikov, D. S.; et al. Low-threshold stimulated emission using colloidal quantum wells. *Nano Lett.* **2014**, 14 (5), 2772–2777.
- (31) Guzelturk, B.; Kelestemur, Y.; Olutas, M.; Delikanli, S.; Demir, H. V. Amplified spontaneous emission and lasing in colloidal nanoplatelets. *ACS Nano* **2014**, *8* (7), 6599–6605.
- (32) Dede, D.; Taghipour, N.; Quliyeva, U.; et al. Highly stable multicrown heterostructures of type-II nanoplatelets for ultralow threshold optical gain. *Chem. Mater.* **2019**, 31 (5), 1818–1826.
- (33) Taghipour, N.; Delikanli, S.; Shendre, S.; Sak, M.; Li, M.; Isik, F.; Tanriover, I.; Guzelturk, B.; Sum, T. C.; Demir, H. V. Sub-single exciton optical gain threshold in colloidal semiconductor quantum wells with gradient alloy shelling. *Nat. Commun.* **2020**, *11* (1), 3305.
- (34) Chen, Z.; Nadal, B.; Mahler, B.; Aubin, H.; Dubertret, B. Quasi-2D colloidal semiconductor nanoplatelets for narrow electroluminescence. *Adv. Funct. Mater.* **2014**, *24* (3), 295–302.
- (35) Kelestemur, Y.; Shynkarenko, Y.; Anni, M.; Yakunin, S.; De Giorgi, M. L.; Kovalenko, M. V. Colloidal CdSe quantum wells with graded shell composition for low-threshold amplified spontaneous emission and highly efficient electroluminescence. *ACS Nano* **2019**, *13* (12), 13899–13909.
- (36) Guo, Y.; Gao, F.; Huang, P.; Wu, R.; Gu, W.; Wei, J.; Liu, F.; Li, H. Light-emitting diodes based on two-dimensional nanoplatelets. *Energy Mater. Adv.* **2022**, 2022, 1–24.
- (37) Tessier, M. D.; Javaux, C.; Maksimovic, I.; Loriette, V.; Dubertret, B. Spectroscopy of single CdSe nanoplatelets. *ACS Nano* **2012**, *6* (8), 6751–6758.
- (38) D'Amato, M.; Fu, N.; Glorieux, Q.; et al. Room-temperature efficient single-photon generation from CdSe/ZnS nanoplatelets. *ACS Nano* **2025**, *19* (14), 14404–14409.
- (39) Liang, X.; Durmusoglu, E. G.; Lunina, M.; et al. Near-unity emitting, widely tailorable, and stable exciton concentrators built from doubly gradient 2D semiconductor nanoplatelets. *ACS Nano* **2023**, *17* (20), 19981–19992.
- (40) Nair, G.; Zhao, J.; Bawendi, M. G. Biexciton quantum yield of single semiconductor nanocrystals from photon statistics. *Nano Lett.* **2011**, *11* (3), 1136–1140.
- (41) Zhao, J.; Chen, O.; Strasfeld, D. B.; Bawendi, M. G. Biexciton quantum yield heterogeneities in single CdSe (CdS) core (shell) nanocrystals and its correlation to exciton blinking. *Nano Lett.* **2012**, 12 (9), 4477–4483.
- (42) Galland, C.; Ghosh, Y.; Steinbrück, A.; et al. Two types of luminescence blinking revealed by spectroelectrochemistry of single quantum dots. *Nature* **2011**, 479 (7372), 203–207.
- (43) Yuan, G.; Gómez, D. E.; Kirkwood, N.; Boldt, K.; Mulvaney, P. Two mechanisms determine quantum dot blinking. *ACS Nano* **2018**, 12 (4), 3397–3405.
- (44) Trinh, C. T.; Minh, D. N.; Ahn, K. J.; Kang, Y.; Lee, K.-G. Verification of type-A and type-B-HC blinking mechanisms of organic—inorganic formamidinium lead halide perovskite quantum dots by FLID measurements. *Sci. Rep.* **2020**, *10* (1), 2172.
- (45) Park, Y.-S.; Bae, W. K.; Pietryga, J. M.; Klimov, V. I. Auger recombination of biexcitons and negative and positive trions in individual quantum dots. *ACS Nano* **2014**, *8* (7), 7288–7296.
- (46) Zhang, Y.; Guo, T.; Yang, H.; Bose, R.; Liu, L.; Yin, J.; Han, Y.; Bakr, O. M.; Mohammed, O. F.; Malko, A. V. Emergence of multiple fluorophores in individual cesium lead bromide nanocrystals. *Nat. Commun.* **2019**, *10* (1), 2930.
- (47) Kuno, M.; Fromm, D. P.; Hamann, H. F.; Gallagher, A.; Nesbitt, D. J. "On"/"off" fluorescence intermittency of single

- semiconductor quantum dots. J. Chem. Phys. **2001**, 115 (2), 1028–1040.
- (48) Peterson, J. J.; Nesbitt, D. J. Modified power law behavior in quantum dot blinking: A novel role for biexcitons and Auger ionization. *Nano Lett.* **2009**, *9* (1), 338–345.
- (49) Kuno, M.; Fromm, D. P.; Hamann, H. F.; Gallagher, A.; Nesbitt, D. J. Nonexponential "blinking" kinetics of single CdSe quantum dots: A universal power law behavior. *J. Chem. Phys.* **2000**, *112* (7), 3117–3120.
- (50) Guo, W.; Tang, J.; Zhang, G.; et al. Photoluminescence Blinking and Biexciton Auger Recombination in Single Colloidal Quantum Dots with Sharp and Smooth Core/Shell Interfaces. *J. Phys. Chem. Lett.* **2021**, *12* (1), 405–412.
- (51) Pietryga, J. M.; Park, Y.-S.; Lim, J.; et al. Spectroscopic and Device Aspects of Nanocrystal Quantum Dots. *Chem. Rev.* **2016**, *116* (18), 10513–10622.

